between the appropriate GCM climates and accounting for the logarithmic radiative effect of CO_2. Unlike the shorter 40-kyr simulations (first step), ice albedo and topographic feedbacks are not calculated explicitly, but the latter are captured by the lapse-rate correction in the mass-balance calculations.

Received 25 July; accepted 12 November 2002; doi:10.1038/nature01290.

1. Zachos, J. C., Quinn, T. M. & Salamy, K. A. High-resolution (10^4 years) deep-sea foraminiferal stable isotope records of the Eocene–Oligocene climate transition. *Paleoceanography* **11,** 251–266 (1996).
2. Zachos, J., Pagani, M., Sloan, L. & Thomas, E. Trends, rhythms, and aberrations in global climate 65 Ma to present. *Science* **292,** 686–693 (2001).
3. Lear, C. H., Elderfield, H. & Wilson, P. A. Cenozoic deep-sea temperatures and global ice volumes from Mg/Ca in benthic foraminiferal calcite. *Science* **287,** 269–272 (2000).
4. Barrett, P. J. Antarctic paleoenvironment through Cenozoic times—a review. *Terr. Antarct.* **3,** 103–119 (1996).
5. Kennett, J. P. Cenozoic evolution of Antarctic glaciation, the circum-Antarctic oceans and their impact on global paleoceanography. *J. Geophys. Res.* **82,** 3843–3859 (1977).
6. Lawver, L. A., Gahagan, L. M. & Coffin, M. F. in *The Antarctic Paleoenvironment: A Perspective on Global Change* (eds Kennett, J. P. & Warnke, D. A.) 7–30 (American Geophysical Union, Washington DC, 1992).
7. Hambrey, M. J., Larsen, B. & Ehrmann, W. U. in *Ocean Drilling Program Scientific Results* 119 (eds Barron, J. & Larsen, B.) 77–132 (College Station, Texas, 1991).
8. Wilson, G. S., Roberts, A. P., Verosub, K. L., Florindo, F. & Sagnotti, L. Magnetobiostratigraphic chronology of the Eocene–Oligocene transition in the CIROS-1 core, Victoria Land margin, Antarctica: Implications for Antarctic glacial history. *Geol. Soc. Am. Bull.* **110,** 35–47 (1998).
9. Zachos, J. C., Breza, J. R. & Wise, S. W. Early Oligocene ice sheet expansion on Antarctica: stable isotope and sedimentological evidence from Kerguelen Plateau, southern Indian Ocean. *Geology* **20,** 569–573 (1992).
10. Ehrmann, W. U. & Mackensen, A. Sedimentologic evidence for the formation of an East Antarctic ice sheet in Eocene/Oligocene time. *Palaeogeogr. Palaeoclimatol. Palaeoecol.* **93,** 85–112 (1992).
11. Francis, J. E. Evidence from fossil plants for Antarctic Paleoclimates over the past 100 million years. *Terr. Antarct. Rep.* **3,** 43–52 (1999).
12. Barrett, P. J., Elston, D. P., Harwood, D. M., McKelvey, B. C. & Webb, P.-N. Mid-Cenozoic record of glaciation and sea-level change on the margin of Victoria Land basin, Antarctica. *Geology* **15,** 634–637 (1987).
13. Naish, T. R. *et al.* Orbitally induced oscillations in the East Antarctic ice sheet at the Oligocene/Miocene boundary. *Nature* **413,** 719–723 (2001).
14. Exon, N., Kennett, J., Malone, M. & the Leg 189 Shipboard Scientific Party. The opening of the Tasmanian gateway drove global Cenozoic paleoclimatic and paleoceanographic changes: results of Leg 189. *JOIDES J.* **26,** 11–17 (2000).
15. Toggweiler, J. R. & Bjornsson, H. Drake Passage and paleoclimate. *J. Quat. Sci.* **15,** 319–328 (2000).
16. Nong, G. T., Najjar, R. G., Seidov, D. & Peterson, W. Simulation of ocean temperature change due to the opening of Drake Passage. *Geophys. Res. Lett.* **27,** 2689–2692 (2000).
17. Lawver, L. A. & Gahagan, L. M. in *Tectonic Boundary Conditions for Climate Reconstructions* (eds Crowley, T. J. & Burke, K. C.) 212–223 (Oxford Univ. Press, New York, 1998).
18. Barker, P. F. & Burrell, J. The opening of Drake Passage. *Mar. Geol.* **25,** 15–34 (1977).
19. Pearson, P. N. & Palmer, M. R. Atmospheric carbon dioxide over the past 60 million years. *Nature* **406,** 695–699 (2000).
20. Pagani, M., Arthur, M. A. & Freeman, K. H. Miocene evolution of atmospheric carbon dioxide. *Paleoceanography* **14,** 273–292 (1999).
21. Birchfield, G. E., Weertman, J. & Lunde, A. T. A model study of the role of high latitude topography in the climatic response to orbital insolation anomalies. *J. Atmos. Sci.* **39,** 71–87 (1982).
22. Abe-Ouchi, A. & Blatter, H. On the initiation of ice sheets. *Ann. Glaciaol.* **18,** 203–207 (1993).
23. Maqueda, M., Willmott, A. J., Bamber, J. L. & Darby, M. S. An investigation of the small ice cap instability in the Southern Hemisphere with a coupled atmosphere–sea ice–ocean–terrestrial ice model. *Clim. Dyn.* **14,** 329–352 (1998).
24. Huybrechts, P. Glaciological modelling of the late Cenozoic East Antarctic ice sheet: stability or dynamism? *Geograf. Annal.* **75,** 221–238 (1993).
25. Thompson, S. L. & Pollard, D. Greenland and Antarctic mass balances for present and doubled atmospheric CO_2 from the GENESIS Version-2 Global Climate Model. *J. Clim.* **10,** 871–900 (1997).
26. Kamb, B. in *The West Antarctic Ice Sheet: Behaviour and Environment* (eds Alley, R. A. & Bindschadler, R. A.) 157–199 (American Geophysical Union, Washington DC, 2001).
27. Clark, P. U. & Pollard, D. Origin of the mid-Pleistocene transition by ice-sheet erosion of regolith. *Paleoceanography* **13,** 1–9 (1998).
28. Brotchie, J. F. & Sylvester, R. On crustal flexure. *J. Geophys. Res.* **74,** 5240–5252 (1969).
29. Ritz, C., Fabre, A. & Letreguilly, A. Sensitivity of a Greenland ice-sheet model to ice flow and ablation parameters: consequences for the evolution through the last climate cycle. *Clim. Dyn.* **13,** 11–24 (1997).
30. Bamber, J. A. & Bindschadler, R. A. An improved elevation dataset for climate and ice-sheet modelling: validation with satellite imagery. *Ann. Glaciol* **25,** 439–444 (1997).

Supplementary Information accompanies the paper on *Nature*'s website (**http://www.nature.com/nature**).

Acknowledgements This material is based upon work supported by the National Science Foundation.

Competing interests statement The authors declare that they have no competing financial interests.

Correspondence and requests for materials should be addressed to R.D. (e-mail: deconto@geo.umass.edu).

Evolution of the Archaean crust by delamination and shallow subduction

Stephen F. Foley*, Stephan Buhre† & Dorrit E. Jacob*

* *Institut für Geologische Wissenschaften, Universität Greifswald, F.L.-Jahnstrasse 17a, 17487 Greifswald, Germany*
† *Institut für Mineralogie, Universität Frankfurt, Senckenberganlage 28, 60054 Frankfurt-am-Main, Germany*

The Archaean oceanic crust was probably thicker than present-day oceanic crust owing to higher heat flow and thus higher degrees of melting at mid-ocean ridges[1]. These conditions would also have led to a different bulk composition of oceanic crust in the early Archaean, that would probably have consisted of magnesium-rich picrite (with variably differentiated portions made up of basalt, gabbro, ultramafic cumulates and picrite). It is unclear whether these differences would have influenced crustal subduction and recycling processes, as experiments that have investigated the metamorphic reactions that take place during subduction have to date considered only modern mid-ocean-ridge basalts[2,3]. Here we present data from high-pressure experiments that show that metamorphism of ultramafic cumulates and picrites produces pyroxenites, which we infer would have delaminated and melted to produce basaltic rocks, rather than continental crust as has previously been thought. Instead, the formation of continental crust requires subduction and melting of garnet-amphibolite[4]—formed only in the upper regions of oceanic crust—which is thought to have first occurred on a large

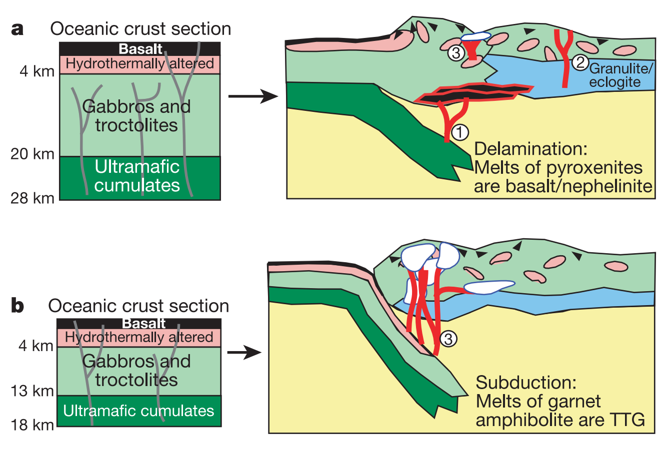

Figure 1 Model for the constitution and fate of oceanic crust. **a**, Hadean/early Archaean; delamination of ultramafic cumulates occurs. **b**, Late Archaean; subduction of the whole ocean crust occurs. Oceanic crust sections are estimated on the basis of eclogite xenolith petrology and chemistry[12–14], and thermodynamic modelling of the fractionation of picrites[15]. Parental picrites fractionate at the crust–mantle boundary to produce about 30% ultramafic cumulates, predominantly olivine and clinopyroxene. Grey lines indicate that more picritic melts are thought to have approached the surface in the Archaean[13,16]. Melts may be produced by three main processes: in the Hadean and early Archaean, the metamorphosed ultramafic cumulates (now pyroxenites—see Fig. 2c) delaminate and melt to produce basaltic to nephelinitic melts which are greatly different from early continental crust (process 1). The lower crust may melt as eclogite[10] (process 2), but only after removal of the lower ultramafic cumulate layer. The production of melts from garnet-amphibolites (process 3) is needed to produce continental-crust-like TTG suite[4]; this must have been rare (although not absent) in the early Archaean before the subduction of the hydrothermally altered uppermost basaltic crustal layer, but became important once the whole crust could be subducted[20].

scale during subduction in the late Archaean[5]. We deduce from this that shallow subduction and recycling of oceanic crust took place in the early Archaean, and that this would have resulted in strong depletion of only a thin layer of the uppermost mantle. The misfit between geochemical depletion models and geophysical models for mantle convection (which include deep subduction) might therefore be explained by continuous deepening of this depleted layer through geological time[5,6].

No unequivocal samples of Archaean oceanic crust are preserved at Earth's surface, so that processes surrounding the subduction and recycling of Archaean oceanic crust remain obscure. Indirect clues come from the preserved early continental crust, which broadly corresponds to tonalite–trondhjemite–granodiorite gneisses (TTG)[7]. These gneisses formed by partial melting of either eclogitic or amphibolitic oceanic crust[8–10]. However, recent trace-element partitioning results show that the paired low Nb/Ta ratio and high Zr/Sm ratio of TTG must have formed by melting of garnet-amphibolite, and not eclogite[4]. The occurrence and melting of eclogite and/or garnet-amphibolite in the oceanic crust is therefore of central importance to assessing Archaean processes. Here, we consider where and when melting of garnet-amphibolite could have occurred in the Archaean oceanic setting.

The interpretation of greenstone belts as oceanic crust is not uncommon, but controversial[1], and if oceanic, they may be formed by the accretion of marginal basins and not represent crust of the open ocean[11]. We prefer to consider eclogite xenoliths carried to the surface by kimberlites, as these may provide the only direct samples of crust formed in Archaean ocean basins. Many of these eclogites may be of late Archaean age, judging by the age determinations currently available (3.0–2.5 Gyr; refs 12–14). Those representing former volcanic rocks are picrites with more MgO than modern mid-ocean-ridge basalts (MORB; 5–8%) but considerably less MgO than komatiites. We interpret this to mean that the bulk oceanic crust was not komatiitic at any time after the Hadean era.

Figure 1 presents a model for the Archaean oceanic crust based on evidence from the eclogite suites and on thermodynamic calculations of the fractionation of picritic melts[15]. Owing to continual cooling of the Earth, the oceanic crust thinned from in excess of 25 km at about 3.5 Gyr ago to less than 20 km at 2.5 Gyr ago. The best modern analogues for such thick crust are oceanic plateaux[10,15], but these are not directly comparable as they form by near-stationary plume activity and not at spreading ridges. Oceanic plateaux are modelled as comprising ultramafic cumulates and basalt–gabbro–troctolite fractionates in a thickness ratio of about 1:3 from picritic parental melts[15]. Thus, an 18-km-thick crust would have 12–13 km basalt and gabbro above ultramafic cumulates consisting mostly of olivine and pyroxene[15] (Fig. 1). However, recent studies of high-level gabbros in the oceanic crust show that primitive melts can approach the surface in modern fast-spreading ridges[16], so that more rapid extension in the Archaean may have led to more picritic components in the upper parts of the crust than on oceanic plateaux today. Many eclogite xenoliths are the metamorphic products of gabbro protoliths, in agreement with fractionation models showing that basaltic residual melts should be widespread[15].

Furthermore, ridge melts generally have very low water contents, as do plume-related melts[17], so that the formation of amphibolite on metamorphism of basaltic fractionates would be limited to the uppermost hydrothermally altered oceanic crust, probably 3–4 km depth[1]. Below this, granulites and eclogites would dominate. An important time constraint is that TTG melt production requires melting of the hydrothermally altered uppermost oceanic crust as garnet-amphibolite[4].

The behaviour of modern MORB during subduction metamorphism is well studied experimentally[2,3], whereas no studies on picrites have been undertaken (to our knowledge). Therefore, we have conducted high-pressure experiments on a lava from Gorgona island, Colombia, with 17.5 wt% MgO (Table 1). MORB transforms with increasing pressure from granulite to garnet-granulite at 1.0–1.2 GPa depending on temperature, and then to eclogite at 1.5–1.7 GPa owing to the elimination of plagioclase. If wet, these rocks correspond to amphibolite, garnet-amphibolite and eclogite

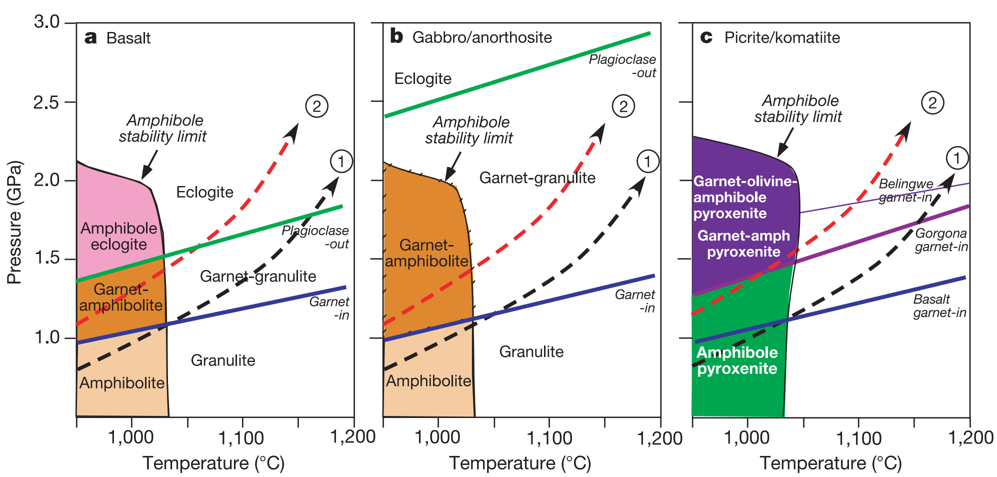

Figure 2 Stability of metamorphic products of parts of the Archaean oceanic crust. Coloured regions represent rocks produced by subduction metamorphism of **a**, MORB[2,3], **b**, gabbro/anorthosite, corresponding to plagioclase-rich plutonic rocks[2], and **c**, the Gorgona composition studied here. Garnet is stable above the 'garnet-in' curves, which lie at similar pressures for MORB and anorthosite, but at higher pressures with increasing MgO content for Gorgona and Belingwe komatiite (26.5% MgO; S.B., unpublished data). Garnet-granulite has widely differing stability fields in **a** and **b**, but does not occur at all in **c**. Melting points do not change much as a function of the MgO content of the rock wherever amphibole is present (phase relations interpolated after refs 29 and 30); melting occurs where the geotherms (dashed lines showing schematically conditions for early (geotherm 1) and late (geotherm 2) Archaean) pass out of the (coloured) regions of subsolidus rocks. The Gorgona rock (**c**) melts along subduction geotherm 1 as amphibole–pyroxenite (dark green)—neither garnet nor plagioclase are stable—and along geotherm 2 as a garnet and amphibole-bearing pyroxenite (purple). The metamorphic equivalents of picrites and ultramafic cumulates are too MgO-rich to contain plagioclase during subduction. Formation of TTG gneisses requires melting of garnet-amphibolite[4], which occurs for both basalt and gabbro/anorthosite (**a**, **b**), but only after cooling to conditions colder than geotherm 1. This prevents widespread formation of TTG with low Nb/Ta in the early Archaean; this must await a general thinning of the oceanic crust until the hydrothermally altered basaltic upper levels can be subducted and transform to amphibolite. No TTG-like melts can be produced by melting picrites or ultramafic cumulates under any conditions (**c**).

at lower temperatures (Fig. 2a). For plagioclase-rich cumulates, the fields for garnet- and plagioclase-bearing rocks extend to much higher pressures, but begin at about the same depth (Fig. 2b). Our results show that the metamorphic products of picrites or ultramafic cumulates (dark green and grey in Fig. 1) are plagioclase-free, and that the incoming of garnet lies at higher pressures than for MORB (1.7 GPa at 1,100 °C; Fig. 2c). These rocks can never transform to eclogite or garnet-amphibolite under subsolidus conditions, but will transform to rocks bearing orthopyroxene and/or olivine. Water-bearing equivalents are amphibole–pyroxenite, garnet-amphibole–pyroxenite, and garnet-olivine-amphibole–pyroxenite with increasing pressure (Fig. 2c). Partial melts of none of these pyroxenites will correspond to TTG or any other continental-crust-like composition, but will produce melts that are essentially basaltic, even if wet[18]. Also, these rocks may not undergo the sudden increase in density experienced by basalts during the granulite–eclogite transformation[2].

Subduction geotherms during the Archaean era are very poorly known, but will have been disproportionately hotter than modern ones owing to the dominance of smaller plates that were younger and hotter on subduction than today[19]. The eclogite xenoliths have very low Nb/Ta ratios indicating strong source depletion, and are reminiscent of a 'subduction zone' geochemical signature[13] fitting a model with small plates and common ridge–subduction interaction[19]. Schematic geotherms are shown in Fig. 2; geotherm 1 would apply to the early Archaean, whereas geotherm 2 represents conditions in the latest Archaean. The following tectonic model is consistent with our experiments and the melting of other rock types in subduction zones, and with the production rates of TTG and early continental crust[5]. In the early Archaean, the crust was too thick to be subducted as a unit[20], and so the lower parts were delaminated and melted (Figs 1 and 2c). Melts of these metamorphosed ultramafic cumulates, now pyroxenites (Fig. 2c), are basaltic to nephelinitic[18], and so the production of voluminous TTG-like melts was not favoured in Archaean subduction-like settings.

The oceanic crust became steadily thinner until, in the late Archaean (3.3–3.0 Gyr ago), a threshold was reached after which the whole crust could be subducted[20]. At this time, the hydrothermally altered uppermost 4 km of crust was introduced into the subduction zone, and basaltic rocks were subject to widespread melting as garnet-amphibolite (Fig. 2a, b). Now, large volumes of TTG-like melts with high Zr/Sm and low Nb/Ta (ref. 4) could be produced for the first time, explaining the increase in volume of continental crust preserved from the late Archaean[5]. TTG melts could be produced during the delamination period of the early Archaean (Fig. 1) only from eclogitic lower crust from which the ultramafic cumulates had already been removed (process 2 in Fig. 1), or by melting of amphibolite within the thick crust (process 3 in Fig.1). Partial melting of eclogite is commonly invoked to produce TTG[10], but would have to await delamination of the cumulate pile and so removal of the thermal protection from mantle temperatures. Furthermore, melting of eclogites in the lower parts of thick oceanic crust would produce rocks of broadly TTG composition in terms of major elements[8,9], but which do not have low Nb/Ta (ref. 4); these are not thought to be common in the geological record[7].

At any one time, the thickness and make-up of the oceanic crust and its age at subduction will have varied, so that TTG were produced, but only in small volumes, in the early Archaean[21]. We conclude that the melting of garnet-amphibolite required for TTG production[4] first became dominant in subducting slabs after about 3.2 Gyr ago. This corresponds to the first appearance of eclogite xenoliths with oceanic-crust signatures[12–14], and trace-element distributions demonstrate that many of these eclogites result from solid-state transformation of partially melted garnet-amphibolite[4].

Although eclogite transformation[2] is largely discredited as the main driving force for subduction on the modern Earth[22], it may have served to help initiate the modern style of subduction. The calculated density for the amphibole-bearing Gorgona composition increases from 3.29 to only 3.36 g cm^{-3} across the 'garnet-in' curve, and gradually to 3.53 g cm^{-3} at 1.8 GPa owing to increase of the modal abundance ratio of garnet to amphibole. Large density differences (0.5–0.6 g cm^{-3}) first occur when basaltic and gabbroic rocks dominate the subducting part of the crust, initially by allowing transformation of garnet-amphibolite into eclogite by partial melting.

Thus, until the latest Archaean the contribution of the down-going oceanic crust to slab pull was minimal. Also, subducting slabs were hotter and the subduction angle flatter than today[19], so deep subduction may not have existed until eclogite-bearing slabs helped to pull the near-surface slabs deeper. Calculations show that the increased importance of chemical buoyancy in young, hot slabs tends to inhibit deep penetration[23]. Only after slabs cooled further,

Table 1 **High-pressure experiments on the Gorgona komatiite composition**

Experiment	Pressure (GPa)	Temperature (°C)	Duration (h)	Phases observed
SB-8	1.5	950	168	am + cpx + opx + gt + sp
SB-11	1.8	950	170	am + cpx + opx + gt + sp
SB-23	1.0	1,000	168	am + cpx + opx + sp
SB-26	1.2	1,000	170	am + cpx + opx + sp
SB-14	1.4	1,000	168	am + cpx + opx + gt
SB-16	1.6	1,000	169	am + cpx + opx + gt + ol
SB-15	1.8	1,000	168	am + cpx + opx + gt + ol
SB-35	1.2	1,150	144	cpx + opx + ol + sp + melt
SB-17	1.6	1,150	168	cpx + opx + ol + sp + melt
SB-18	1.8	1,150	168	cpx + opx + gt + ol + melt
SB-21	2.0	1,150	161	cpx + opx + gt + ol + melt
SB-25	2.5	1,150	168	cpx + gt + ol + melt

Abbreviations for phases: am, amphibole: cpx, clinopyroxene: opx, orthopyroxene; gt, garnet; sp, spinel; ol, olivine. The starting material for high-pressure experiments was prepared as a glass from Gorgona komatiite sample GOR-94-1, donated by C. Ginibre. The composition of the glass (wt%) is SiO_2 46.3, TiO_2 0.66, Al_2O_3 10.1, FeO 11.57, MgO 17.5, CaO 10.2, Na_2O 1.24, K_2O 0.03, Cr_2O_3 0.10, Mg# 73.0. Experiments were run in a piston-cylinder apparatus with CaF_2 as pressure medium. Pt capsules with graphite inner sleeves were used, and experiments were run in water-undersaturated conditions (0.2–0.3 wt% H_2O).

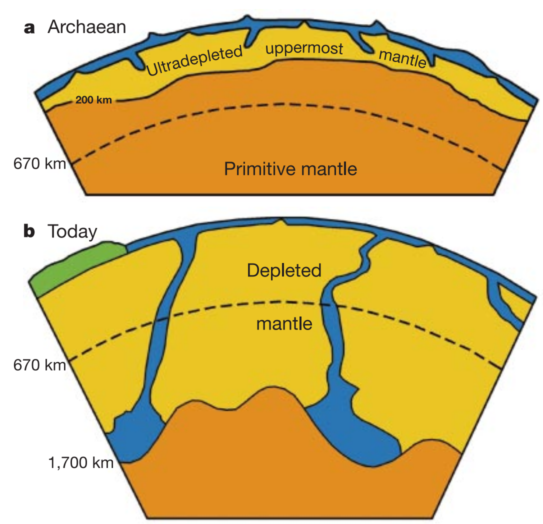

Figure 3 Model for progressive deepening of the depleted mantle with time. In contrast to the modern picture (**b**) where deep subduction drives the vestiges of plates into the lower mantle[26,27], the early Archaean oceanic crust (**a**) may have been produced from a layer restricted to the uppermost 200 km that consequently became strongly depleted. Only the ultramafic lower crust was returned to the mantle, and melted once again to produce more basalt. Only after thinning of the oceanic crust allowed widespread transformation of basaltic upper crust into eclogite via partial melting at the end of the Archaean may eclogite have helped to initiate the modern subduction style. Evidence for this is seen in ultradepleted trace elements in eclogite xenoliths[13], all of which are between 3.0 and 2.6 Gyr old[12–14], and in fractionated Nd isotopes in the early Archaean[5,6].

and the olivine–spinel transition was reached in the underlying peridotite part of the subducting slab, could the subduction process develop into one similar to that operating today.

Evidence for this depth restriction of subduction and shallow return of crustal components to the mantle may be found in the low Nb/Ta and Zr/Hf ratios of eclogite xenoliths[13]. These are more depleted than expected for the modern Earth, and are in marked contrast to the high values presumed to represent eclogite in mixing models between depleted mantle and recycled eclogites[24]. This apparent contradiction is resolved if the eclogite xenoliths were indeed relatively enriched for the oceanic crust of the time, but the complementary ultradepleted upper mantle was later eliminated by remixing.

Taken together, the evidence presented here supports a plate model in which only the uppermost 200 km of the mantle were tapped by oceanic volcanism in the early Archaean (Fig. 3a), as has been proposed to account for the fractionation of Nd isotopes in the early Archaean[5,6]. This may have interesting consequences for mass-balance models between crust and mantle: geochemical models have favoured depletion of about 50% of the whole mantle to produce the crust[25], but are at odds with recent geophysical models for subduction into the lower mantle[26]. Given that seismic tomography images can picture only the state of the mantle today, the geochemically modelled 50% depletion of the mantle may be a time-integrated effect of the progressive deepening of the effective depth of the mantle involved in the development of the crust. This was restricted to the uppermost 200 km in the early Archaean[5,6], and today involves large parts of the lower mantle[27] (Fig. 3b). □

Methods

Density calculations were performed by fitting linear interpolations from end-member minerals to microprobe analyses of experimental minerals, correcting for thermal expansion and compressibility[28], and combining with modal mineral analyses from the experiments.

Received 11 March; accepted 19 November 2002; doi:10.1038/nature01319.

1. Bickle, M. J., Nisbet, E. G. & Martin, A. Archean greenstone belts are not oceanic crust. *J. Geol.* **102,** 121–138 (1994).
2. Green, D. H. & Ringwood, A. E. An experimental investigation of the gabbro to eclogite transformation and its petrological applications. *Geochim. Cosmochim. Acta* **31,** 767–833 (1967).
3. Schmidt, M. W. & Poli, S. Experimentally based water budgets for dehydrating slabs and consequences for arc magma generation. *Earth Planet. Sci. Lett.* **163,** 361–379 (1998).
4. Foley, F., Tiepolo, M. & Vannucci, R. Growth of early continental crust in subduction zones controlled by melting of amphibolite. *Nature* **417,** 837–840 (2002).
5. McCulloch, M. T. & Bennett, V. C. Progressive growth of the Earth's continental crust and depleted mantle: geochemical constraints. *Geochim. Cosmochim. Acta* **58,** 4717–4738 (1994).
6. Bennett, V. C., Nutman, A. P. & McCulloch, M. T. Nd isotopic evidence for transient, highly depleted mantle reservoirs in the early history of the Earth. *Earth Planet. Sci. Lett.* **119,** 299–317 (1993).
7. Martin, H. in *Archean Crustal Evolution* (ed. Condie, K. C.) 205–259 (Elsevier, Amsterdam, 1994).
8. Winther, K. T. & Newton, R. C. Experimental melting of hydrous low-K tholeiite: evidence on the origin of Archaean cratons. *Bull. Geol. Soc. Denmark* **39,** 213–228 (1991).
9. Rapp, R. P., Watson, E. B. & Miller, C. F. Partial melting of amphibolite/eclogite and the origin of Archean trondhjemites and tonalites. *Precambr. Res.* **51,** 1–25 (1991).
10. Zegers, T. E. & van Keken, P. E. Middle Archean continent formation by crustal delamination. *Geology* **29,** 1083–1086 (2001).
11. de Wit, M. J. & Ashwal, L. D. (eds) *Greenstone Belts* (Oxford Univ. Press, Oxford, 1996).
12. Jacob, D., Jagoutz, E., Lowry, D., Mattey, D. & Kudryatseva, G. Diamondiferous eclogites from Siberia: remnants of Archean oceanic crust. *Geochim. Cosmochim. Acta* **58,** 5191–5207 (1994).
13. Jacob, D. E. & Foley, S. F. Evidence for Archean oceanic crust with low high field strength element signature from diamondiferous eclogite xenoliths. *Lithos* **48,** 317–336 (1999).
14. Shirey, S. B. *et al.* Archean emplacement of eclogitic components into the lithospheric mantle during formation of the Kaapvaal craton. *Geophys. Res. Lett.* **28,** 2509–2512 (2001).
15. Farnetani, C. G., Richards, M. A. & Ghiorso, M. S. Petrological models of magma evolution and deep crustal structure beneath hotspots and flood basalt provinces. *Earth Planet. Sci. Lett.* **143,** 81–94 (1996).
16. Coogan, L. A., Thompson, G. & MacLeod, C. J. A textural and geochemical investigation of high level gabbros from the Oman ophiolite: implications for the role of the axial magma chamber at fast spreading ridges. *Lithos* **63,** 67–82 (2002).
17. Danyushevsky, L. V., Eggins, S. M., Falloon, T. J. & Christie, D. M. H_2O abundance in depleted to moderately enriched mid-ocean ridge magmas; Part I: incompatible behaviour, implications for mantle storage, and origin of regional variations. *J. Petrol.* **41,** 1329–1364 (2001).
18. Foley, S. F., Musselwhite, D. S. & van der Laan, S. R. in *Proc. VIIth Kimberlite Conf.* Vol. 1 (eds Gurney, J. J., Gurney, J. L., Pascoe, M. D. & Richardson, S. H.) 238–246 (Red Roof Design, Cape Town, 1999).
19. Karsten, J. L., Klein, E. M. & Sherman, S. B. Subduction zone geochemical characteristics in ocean ridge basalts from the southern Chile ridge: implications of modern ridge subduction systems for the Archean. *Lithos* **37,** 143–161 (1996).
20. Abbott, D. & Mooney, W. The structural and geochemical evolution of the continental crust: support for the oceanic plateau model of continental growth. *Rev. Geophys. Suppl.* 231–242 (1995).
21. Nutman, A. P., McGregor, V. R., Friend, C. R. L., Bennett, V. C. & Kinny, P. D. The Itsaq Gneiss Complex of southern west Greenland; the world's most extensive record of early crustal evolution (3900-3600 Ma). *Precambr. Res.* **78,** 1–39 (1996).
22. Oxburgh, E. R. & Parmentier, E. M. Compositional and density stratification in oceanic lithosphere—causes and consequences. *J. Geol. Soc. Lond.* **133,** 343–355 (1977).
23. Christensen, U. R. Influence of chemical buoyancy on the dynamics of slabs in the transition zone. *J. Geophys. Res.* **102,** 22435–22443 (1997).
24. Niu, Y. & Batiza, R. Trace element evidence from seamounts for recycled oceanic crust in the Eastern Pacific mantle. *Earth Planet. Sci. Lett.* **148,** 471–483 (1997).
25. O'Nions, R. K., Evensen, N. M. & Hamilton, P. J. Differentiation and evolution of the mantle. *Phil. Trans. R. Soc. Lond. A* **297,** 479–493 (1980).
26. Widiyantoro, S. & van der Hilst, R. Structure and evolution of lithospheric slab beneath the Sunda arc, Indonesia. *Science* **271,** 1566–1570 (1996).
27. Kellogg, L. H., Hager, B. H. & van der Hilst, R. D. Compositional stratification in the deep mantle. *Science* **283,** 1881–1884 (1999).
28. Holland, T. J. B. & Powell, R. An internally consistent thermodynamic data set for phases of petrological interest. *J. Metamorph. Geol.* **16,** 309–343 (1998).
29. Liu, J., Bohlen, S. R. & Ernst, W. G. Stability of hydrous phases in subducting oceanic crust. *Earth Planet. Sci. Lett.* **143,** 161–171 (1996).
30. Wallace, M. E. & Green, D. H. The effect of bulk rock composition on the stability of amphibole in the upper mantle: implications for solidus positions and mantle metasomatism. *Mineral. Petrol.* **44,** 1–19 (1991).

Acknowledgements This Letter is dedicated to the memory of M. Rosenhauer, who prompted the initiation of the experimental programme. This work was supported by the Deutsche Forschungsgemeinschaft.

Competing interests statement The authors declare that they have no competing financial interests.

Correspondence and requests for materials should be addressed to S.F. (e-mail: sfoley@uni-greifswald.de).

Discovery of abundant hydrothermal venting on the ultraslow-spreading Gakkel ridge in the Arctic Ocean

H. N. Edmonds*, P. J. Michael†, E. T. Baker‡, D. P. Connelly§, J. E. Snow‖, C. H. Langmuir¶, H. J. B. Dick#, R. Mühe☆, C. R. German§ & D. W. Graham**

** The University of Texas at Austin, Marine Science Institute, 750 Channel View Drive, Port Aransas, Texas 78373-5015, USA*
† The University of Tulsa, 600 College Avenue, Tulsa, Oklahoma 74104, USA
‡ Pacific Marine Environmental Laboratory, National Oceanic and Atmospheric Administration, 7600 Sand Point Way NE, Seattle, Washington 98115, USA
§ Southampton Oceanography Centre, Southampton SO14 3ZH, UK
‖ Max-Planck Institut für Chemie, Postfach 3060, 55020 Mainz, Germany
¶ Department of Earth and Planetary Sciences, Harvard University, 20 Oxford Street, Cambridge, Massachusetts 02138, USA
 # Department of Marine Geology and Geophysics, Woods Hole Oceanographic Institution, Woods Hole, Massachusetts 02543, USA
☆ University of Kiel, Institute of Geosciences, Olshausenstrasse 40, 24118 Kiel, Germany
*** College of Oceanic and Atmospheric Sciences, Oregon State University, Corvallis, Oregon 97331, USA*

Submarine hydrothermal venting along mid-ocean ridges is an important contributor to ridge thermal structure[1], and the global distribution of such vents has implications for heat and mass fluxes[2] from the Earth's crust and mantle and for the biogeography of vent-endemic organisms.[3] Previous studies have predicted that the incidence of hydrothermal venting would be extremely low on ultraslow-spreading ridges (ridges with full spreading rates <2 cm yr^{-1}—which make up 25 per cent of the global ridge length), and that such vent systems would be hosted in ultramafic in addition to volcanic rocks[4,5]. Here we present evidence for

